NMR Studies of Ligand Carboxylate Group Interactions with Arginine Residues in Complexes of *Lactobacillus casei* Dihydrofolate Reductase with Substrates and Substrate Analogues[†]

Berry Birdsall,[‡] Vladimir I. Polshakov,[‡,§] and James Feeney*[,‡]

Molecular Structure Division, National Institute for Medical Research, The Ridgeway, Mill Hill, London NW7 1AA, U.K., and Center for Drug Chemistry, Moscow 119815, Russia

ABSTRACT: In a series of complexes of *Lactobacillus casei* dihydrofolate reductase (DHFR) formed with substrates and substrate analogues, the ^{1}H/^{15}N NMR chemical shifts for the guanidino group of the conserved Arg 57 residue were found to be sensitive to the mode of binding of their H$^\eta$ protons to the charged oxygen atoms in ligand carboxylate groups. In all cases, Arg 57 showed four nonequivalent H$^\eta$ signals indicating hindered rotation about the N$^\epsilon$−C$^\zeta$ and C$^\zeta$−N$^\eta$ bonds. The H$^{\eta12}$ and H$^{\eta22}$ protons have large downfield shifts as expected for a symmetrical end-on interaction with the ligand carboxylate group. The chemical shifts are essentially the same in the complexes with folate and *p*-aminobenzoyl-L-glutamate (PABG) and similar to those found previously for the methotrexate complex reflecting the strong and similar hydrogen bonds formed with the carboxylate oxygens. Interestingly, the rates of rotation about the N$^\epsilon$−C$^\zeta$ bond for the complexes containing the weakly binding PABG fragment are almost identical to those measured in the complex with methotrexate, which binds 10^7 times more tightly. In the methotrexate complex, this rotation depends on correlated rotations about the N$^\epsilon$−C$^\zeta$ bond of Arg 57 and the C$^\alpha$−C$'$ bond of the ligand glutamate α-carboxylate group. Thus, even in a fragment such as PABG, which has a much faster off-rate, the carboxylate group binds to the enzyme in a similar way to that in a parent molecule such as folate and methotrexate with the rotation about the N$^\epsilon$−C$^\zeta$ bond of Arg 57 being essentially the same in all the different complexes.

NMR is proving to be a very effective method for characterizing hydrogen bonding and electrostatic interactions between the guanidino NH groups of arginine residues in proteins and anionic groups in bound ligand molecules (*1*−*5*). For example, in complexes of SH2 domains formed with bound phosphopeptides, several important arginine−ligand interactions between arginine H$^\eta$ hydrogens and the phosphorylated tyrosines have been detected (*2*−*4*). Interactions involving guanidino groups have also been characterized in complexes of *Lactobacillus casei* dihydrofolate reductase (DHFR)[1] between a conserved arginine residue (Arg 57) and carboxylate groups in antifolate agents such as methotrexate

(*5*) and several brodimoprim analogues (*6*). Previous studies have been aimed at identifying the arginine guanidino H$^\eta$ hydrogens specifically involved in the interactions and characterizing the dynamic processes of the interacting groups in the complex (*5*−*7*). In ^{1}H/^{15}N HSQC spectra of proteins, the H$^\eta$ signals from most of the arginine residues appear as a group of broad unresolved signals in the ^{1}H/^{15}N region 6.0−7.5 ppm/70−76 ppm corresponding to the four H$^\eta$ protons and two N$^\eta$ nitrogens in the arginine guanidino NH$_2$ groups. Some peaks are coalesced signals arising from exchange between the nuclei caused by rotations about the N$^\epsilon$−C$^\zeta$ and C$^\zeta$−N$^\eta$ bonds. Large downfield ^{1}H chemical shifts (∼3 ppm) are observed for guanidino NH groups involved in hydrogen bonding interactions. For example, in a study of the complex of *L. casei* DHFR with methotrexate, four separate H$^\eta$ signals were observed for the Arg 57 residue (Figure 1a and Table 1) indicating hindered rotation in its guanidino group (*5*) and strong hydrogen bond interactions with two of the H$^\eta$ protons. The observed ^{1}H and ^{15}N chemical shifts indicated that the Arg 57 guanidino group interacts with the α-carboxylate group of the glutamate moiety of methotrexate in an symmetrical end-on fashion (see structure in Figure 2) (*5*, *8*). From temperature-dependent line shape changes of the H$^\eta$ signals and from results of zz-HSQC exchange experiments, the rates of rotation about the N$^\epsilon$−C$^\zeta$ and C$^\zeta$−N$^\eta$ bonds were determined and shown to indicate the presence of correlated rates of rotation about the N$^\epsilon$−C$^\zeta$ bond of Arg 57 and the C$^\alpha$−C$'$ bond in the glutamate moiety of bound methotrexate (see Figure 2) (*7*).

* To whom correspondence should be addressed: Dr. J. Feeney, Molecular Structure Division, National Institute for Medical Research, The Ridgeway, Mill Hill, London NW7 1AA. Phone: +44 20 8959 3666. Fax: + 44 20 8906 4477. E-mail: jfeeney@nimr.mrc.ac.uk.

[‡] National Institute for Medical Research.

[§] Center for Drug Chemistry.

[1] Abbreviations: BDM-4, brodimoprim-4-carboxylate; BDM-4,6, brodimoprim-4,6-dicarboxylate; DAP, 2,4-diaminopyrimidine; DHFR, dihydrofolate reductase; DSS, sodium 2,2-dimethyl-2-silapentane-5-sulfonate; GARP, a broad-band decoupling sequence; HSQC, heteronuclear single quantum coherence spectroscopy; MTX, methotrexate; NMR, nuclear magnetic resonance; NOE, nuclear Overhauser effect; NOESY, nuclear Overhauser effect spectroscopy; PABG, *p*-aminobenzoyl-L-glutamate (Scheme 1); ROESY, rotating frame nuclear Overhauser effect spectroscopy; TOCSY, total correlation time spectroscopy; 3D, three-dimensional; 2D, two-dimensional; 2D zz-HSQC, zz-magnetization exchange HSQC spectroscopy.
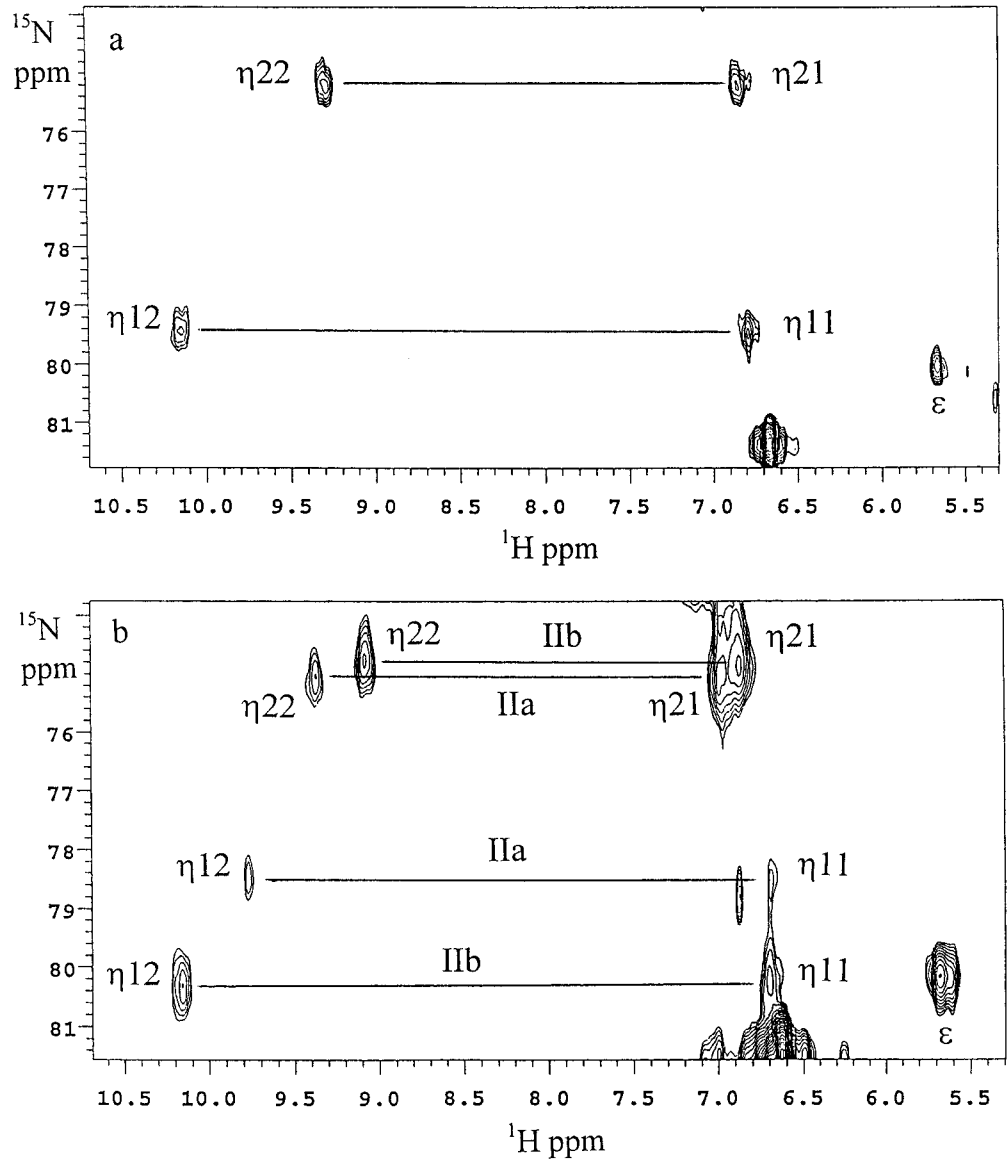
FIGURE 1: Part of the ^{1}H/^{15}N HSQC spectrum recorded at 274 K for complexes of *L. casei* DHFR with (a) methotrexate (at 600 MHz, pH 6.5, and 1 mM) and (b) folate and NADP$^+$ (at 500 MHz, pH 7.3, and 1.2 mM). Complexes contained one equivalent of each ligand. At this pH, two conformations of the folate-NADP$^+$ complex predominate, Forms IIa and IIb. The major differences between the forms are the tautomeric states and the orientations of the folate pterin rings ($\sim$180° difference) (*25, 26*).

Table 1: ^{1}H and ^{15}N Chemical Shifts (ppm) for Arg 57 Guanidino NH Signals in DHFR Complexes with Substrates and Substrate Analogs[a]

DHFR complex	PABG	PABG + DAP	folate + NADP$^+$ Form I	folate + NADP$^+$ Form IIa	folate + NADP$^+$ Form IIb	folate Form a	folate Form b	MTX	MTX	MTX + NADPH	BDM-4	BDM-4,6
pH	6.5	6.5	5.3	7.3	7.3	7.3	7.3	6.5	6.5	6.5	6.5	6.5
temp °C	1	1	1	1	1	1	1	1	35	35	35	35
N$^\epsilon$	80.26	80.34	80.15	80.26	80.26	79.97	79.97	80.05	79.90	80.20	81.91	82.05
H$^\epsilon$	5.67	5.70	5.64	5.66	5.66	5.63	5.63	5.67	5.66	5.62	5.85	5.99
N$^{\eta 1}$	79.88	80.20	78.20	78.47	80.24	78.36	79.65	79.46	79.00	78.60	75.42	77.10
H$^{\eta 11}$	6.99	6.86	6.68	6.68	6.70	6.90	6.90	6.79	6.77	6.55	6.70	6.83
H$^{\eta 12}$	10.18	10.51	10.00	9.77	10.16	9.75	10.09	10.15	10.17	10.00	7.91	8.71
N$^{\eta 2}$	75.65	74.97	75.45	74.91	74.67	75.92	76.27	75.25	75.00	75.20	75.33	73.84
H$^{\eta 21}$	7.00	6.87	7.10	6.97	6.88	7.01	7.01	6.86	6.89	6.87	6.79	6.89
H$^{\eta 22}$	9.34	9.28	9.47	9.37	9.07	9.39	9.55	9.30	9.33	9.33	7.87	7.36

[a] The ^{1}H and ^{15}N chemical shifts are referenced to DSS (sodium 2,2-dimethyl-2-silapentane-5-sulfonate) and liquid NH$_3$, respectively.

The presence of correlated rotations was deduced from the relative rates of rotation about these two bonds that are reversed in the protein complexes as compared with their values in free arginine (*7, 9, 10*). The reversal of the rates could be demonstrated in experiments at 40 °C in which the rate of the N$^\epsilon$−C$^\zeta$ bond rotation (565 $\pm$ 20 s^{-1}) is greater than the measured upper limit for the rate of the C$^\zeta$−N$^\eta$ bond rotation ($<$120 s^{-1}) (data included in Table 2). In this correlated motion model, rotation can take place about the N$^\epsilon$−C$^\zeta$ bond even when the interactions of the guanidino NH$_2$ protons with the carboxylate oxygens remain intact, whereas rotation about a C$^\zeta$−N$^\eta$ bond can only occur when
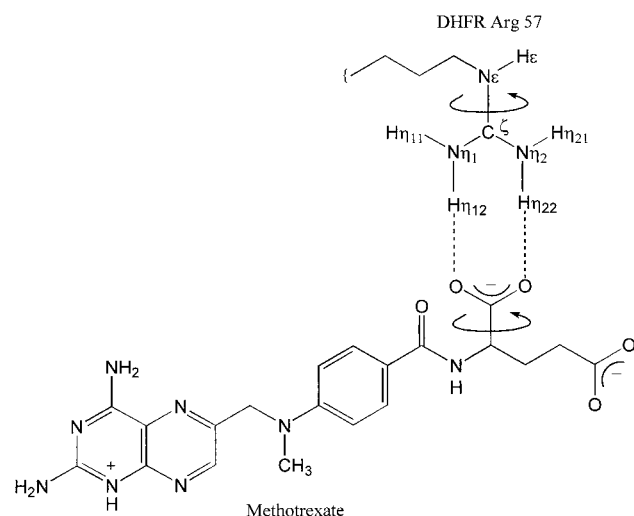
FIGURE 2: Structure of an arginine−carboxylate complex showing the symmetrical end-on interactions of the methotrexate glutamate α-carboxylate group with the guanidino group of Arg 57 of DHFR. Arrows indicate the correlated rotations about the $N^\epsilon-C^\zeta$ bond of Arg 57 and the $C^\alpha-C'$ bond of the glutamate α-carboxylate group of methotrexate.

Table 2: Rates of Rotation (s^{-1}) about the $N^\epsilon-C^\zeta$ and $C^\zeta-N^\eta$ Bonds in Free and Complexed Arginine Residues in DHFR Complexes with Substrates and Substrate Analogues

residue	bond	rate constants (s^{-1})	
		1 °C	40 °C
Arg 57 in DHFR−PABG−DAP	$N^\epsilon-C^\zeta$	13 ± 2[a]	
Arg 57 in DHFR−folate−NADP+ (Form I, pH 5.3)	$N^\epsilon-C^\zeta$	12 ± 3[a]	
Arg 57 in DHFR−folate−NADP+ (Form IIa, pH 7.3)	$N^\epsilon-C^\zeta$	21 ± 3[a]	
Arg 57 in DHFR−folate−NADP+ (Form IIb, pH 7.3)	$N^\epsilon-C^\zeta$	31 ± 3[a]	
Arg 57 in DHFR−MTX	$N^\epsilon-C^\zeta$	14 ± 2[a]	565 ± 20[b]
Arg 57 in DHFR−MTX−NADPH	$N^\epsilon-C^\zeta$	17 ± 4[a,c]	930 ± 100[b]
free arginine[d]	$N^\epsilon-C^\zeta$	110−180[e]	3000−4000[f]
Arg 57 in DHFR−PABG	$C^\zeta-N^\eta$	<200[g]	
Arg 57 in DHFR−PABG−DAP	$C^\zeta-N^\eta$	<60[g]	
Arg 57 in DHFR−folate−NADP+ (Form I, pH 5.3)	$C^\zeta-N^\eta$	<65[g]	
Arg 57 in DHFR−folate−NADP+ (Form IIa, pH 7.3)	$C^\zeta-N^\eta$	<90[g]	
Arg 57 in DHFR−folate−NADP+ (Form IIb, pH 7.3)	$C^\zeta-N^\eta$	<100[g]	
Arg 57 in DHFR−MTX	$C^\zeta-N^\eta$	<110[g]	<120[b]
Arg 57 in DHFR−MTX−NADPH	$C^\zeta-N^\eta$		<70[b]
free N^α-Ac-Arg-O^{i}Pr[h]	$C^\zeta-N^\eta$		26000−53000[h]

[a] From zz-HSQC exchange analysis. [b] From line shape analysis in ref *7*. [c] Extrapolated to 1 °C from rates measured at 15 °C in ref *7* using the activation energy from the DHFR−MTX complex. [d] Data reported in refs *3* and *10*. [e] Extrapolated to 1 °C from rates and activation energies in refs *3* and *10*. [f] Extrapolated to 40 °C from rates and activation energies in refs *3* and *10*. [g] Upper limit determined from two-site line shape analysis. [h] Extrapolated to 40 °C from rates and activation energy for N^α-acetylarginine *iso*-propyl ester in ref *9*.

the interactions with the NH₂ protons are broken. Thus, the rates of rotation about the two bonds will be influenced differently by the rates of hydrogen bond breaking, with the rotation rate for the $C^\zeta-N^\eta$ bond being impeded more than that for the $N^\epsilon-C^\zeta$ bond by the interactions between the arginine guanidino NH₂ protons and the ligand carboxylate groups (*7*). NMR has also been used to identify such interactions in complexes of *L. casei* DHFR formed with a series of analogues of the antibacterial drug trimethoprim [2,4-diamino-5-(3′,5′-dimethoxy-4′-bromobenzyl)pyrimi-

Scheme 1
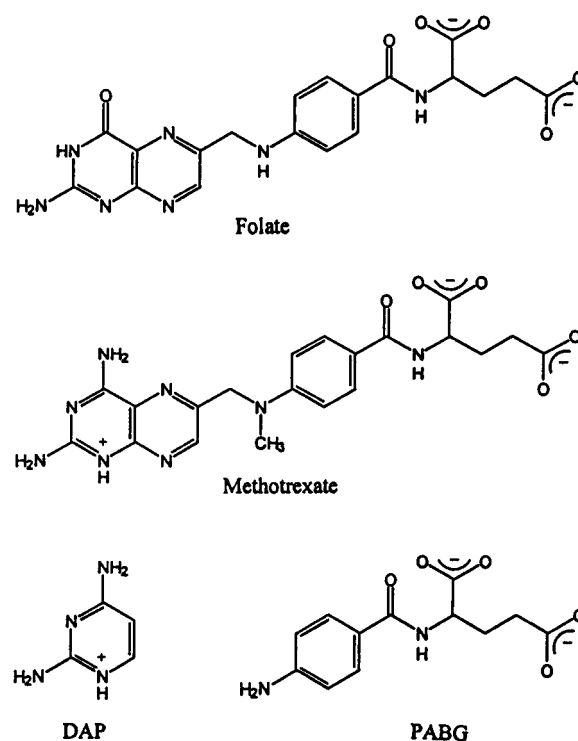
dine] that have substituents at the 3′-O position containing carboxylate groups designed to interact with Arg 57 (*6*).

The aim of the present work is to characterize the structures and dynamics of the Arg 57 guanidino interactions with ligand carboxylate groups in complexes of DHFR with the substrate folate and its fragment, PABG (see Scheme 1). A comparison of the rates of the guanidino bond rotations in different ligand complexes should provide insights into the effects on the dynamics of the individual binding components contributing to the overall set of interactions between the ligand and the protein.

MATERIALS AND METHODS

Materials and Sample Preparation. ¹⁵N-labeled *L. casei* DHFR was expressed in *Escherichia coli* cells grown on a minimal medium and isolated and purified as described previously (*11*, *12*). Folate, methotrexate, NADP+, *p*-aminobenzoyl-L-glutamate (PABG), and 2,4-diaminopyrimidine (DAP) were obtained from Sigma.

Equimolar complexes (~1 mM) of DHFR were formed with folate (binary complex) and folate and NADP+ (ternary complex) and examined by NMR as 0.6 mL samples in 90% H₂O/10% D₂O and 50 mM potassium phosphate, 100 mM KCl, and pH* = 7.3, 6.3, and 5.3 (pH* values are meter readings, unadjusted for deuterium isotope effects). The folate binary complex was prepared by first adding excess folate to the DHFR samples and then dialyzing at pH* 6.5. The pH was adjusted using HCl or KOH solutions as appropriate. The ternary complex was made by adding NADP+ solution to the binary complex, and the sample was examined at pH* = 5.3, 6.3, and 7.3.

The binary complex of DHFR with PABG was prepared by titrating 0.8 mL of a 1.25 mM DHFR solution with aliquots of a concentrated (95 mM) PABG solution and recording the ¹H/¹⁵N HSQC 500 MHz spectrum after each

addition (0.25, 0.46, 0.70, 1.1, 1.8, 2.4, 3.8, and 7.9 equiv). The ternary complex of DHFR with PABG and DAP was prepared by first titrating 1.4 mL of 1.0 mM DHFR (in an 8-mm Shigemi tube) with concentrated PABG solution (0.7, 1.7, 2.9, and 4.4 equiv) and after each addition measuring the $^1H/^{15}N$ HSQC spectrum. At the end of the titrations, the DHFR was 50 to 60% covered with PABG (*13–15*). Three aliquots (0.33, 0.66, and 1.3 equiv) of a DAP solution (18.2 mM) were added to this sample, and $^1H/^{15}N$ HSQC spectra were again recorded after each addition. The DHFR was estimated to be more than 90% covered with each ligand in the ternary complex by monitoring enzyme ^1H signals affected during the titration (*14, 15*). The 1:1 binary DHFR–MTX complex was examined as a 0.6 mL sample (1 mM) in 90% H_2O/10% D_2O and 50 mM potassium phosphate, 100 mM KCl, and pH* 6.5.

NMR Experiments. The NMR experiments were performed at 1–35 °C on Varian 500- and 600-MHz spectrometers. All the NMR experiments used the Watergate technique for water suppression (*16*) and the GARP sequence (*17*) for ^{15}N decoupling during the detection period. Quadrature detection in all indirectly detected dimensions was achieved using the method of States and coworkers (*18*).

The 2D $^1H/^{15}N$ HSQC sequence used in the experiments was essentially the same as that proposed by Mori and coworkers (*19*). The experiments were performed using the following parameters for the ^1H and ^{15}N dimensions respectively: sweep widths 7000–8000 Hz (^1H) and 3600–4000 Hz (^{15}N); 2100–2432 data points (^1H) and 128–180 t_1 increments (^{15}N); processed after zero filling to 4 K (^1H) and 1 K data points (^{15}N). The 2D zz-HSQC experiments (*20, 21*) used in the exchange study on the DHFR–MTX, DHFR–folate–NADP$^+$ and DHFR–PABG–DAP complexes were carried out at 1 °C using a pulse sequence described by Yamazaki and coworkers (*22*). The experiment has a modified gradient enhanced HSQC pulse sequence with a mixing time inserted just prior to the transfer of magnetization from ^{15}N to ^1H. This allows observation of the transference of ^{15}N labeled heteronuclear zz-magnetization (I_zS_z) between the different sites: this experiment was used to connect signals from exchanging species. The experiment was carried out with mixing times of 1–30 ms. The data were processed with zero-filling in both dimensions using Varian software (VNMR, version 5.1). In principle, information about C^ζ–N^η bond rotation rates could be obtained from 3D NOESY–HSQC and ROESY–HSQC experiments. However, in the 3D NOESY–HSQC experiments, there was insufficient sensitivity to detect the diagonal or cross-peaks from the H^η signals.

Rates of bond rotations were also estimated from NMR line shape calculations for two- and three-site exchange processes (including the rates of ligand dissociation where appropriate) using the general multiple site exchange matrix algorithm (*23*). All the calculations and graphical representations of the results were obtained using the program Muses (multiple site exchange simulations), written in-house (*24*)

NMR Signal Assignments. For the binary and ternary complexes of DHFR with PABG and DAP–PABG, the ^1H chemical shift assignments of the H^η signals to Arg 57 could be made in the 3D NOESY–HSQC spectra [at 20 °C (binary) and 35 °C (ternary)] by noting NOEs from the Arg 57 H^ϵ proton to the $H^{\eta 21}$ proton. The H^η chemical shifts of
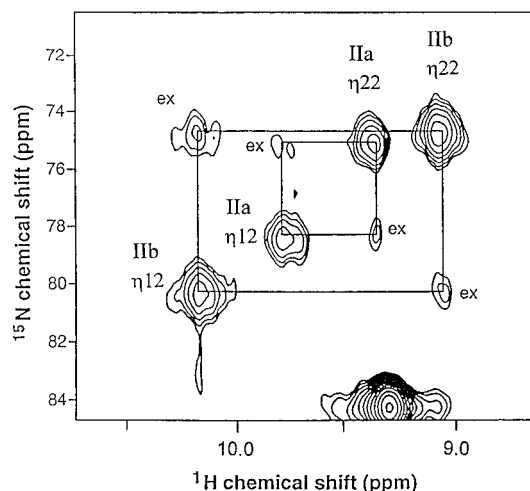

FIGURE 3: Part of the zz-HSQC spectrum recorded with a mixing time of 22 ms, showing the low-field guanidino NH$^\eta$ signals of Arg 57 in the complex of *L. casei* dihydrofolate reductase with folate and NADP$^+$ at pH 7.3. Exchange peaks are indicated by (ex) in the spectrum and allow the connection of the two separate sets of H$^\eta$ signals corresponding to the two conformations Forms IIa and IIb. Major differences between Forms IIa and IIb are the tautomeric states and the orientations of the folate pterin rings (~180° difference).

the four resolved signals for the complexes examined here are all very similar to those of the DHFR–MTX complex, and thus it is possible to make detailed assignments for their H$^\eta$ signals by comparison with the DHFR–MTX results where full assignments have already been made (*5*). The assignments for Arg 57 in the free enzyme have not been made, but the cluster of arginine resonances are observed in the $^1H/^{15}N$ region 6.5–7.4 ppm/70–76 ppm. Table 1 summarizes the ^1H and ^{15}N chemical shifts for nuclei in the guanidino groups of arginine residues in binary and ternary complexes of DHFR with substrates and substrate analogues.

RESULTS

Complexes of DHFR with Folate and NADP$^+$. The ^1H and ^{15}N resonance assignments for the Arg 57 guanidino NH$^\eta$ signals in the DHFR–methotrexate complex made earlier by using 3D $^1H/^{15}N$ TOCSY–HSQC and NOESY–HSQC experiments (*5, 7*) are indicated in Figure 1a. The corresponding region of the $^1H/^{15}N$ HSQC spectrum for the DHFR–folate–NADP$^+$ complex at pH 7.3 presented in Figure 1b, shows two sets of resolved H$^\eta$ signals with very similar chemical shifts to those of the Arg 57 H$^\eta$ signals in the DHFR–methotrexate complex. These signals can be assigned to the two different conformations previously characterized for this complex at high pH, Forms IIa and IIb, where the latter is known to have the larger population (*25, 26*). The signals could be identified as two separate sets of four connected signals by using zz-HSQC experiments. Figure 3 presents the low field part of the spectrum showing cross-peaks between the $\eta 1$ and $\eta 2$ signals in the connected pairs of NH$_2$ groups in each of the two forms. The cross-peaks result from the exchange of the N$^\eta$ magnetization accompanying the slow rotation about the N$^\epsilon$–C$^\zeta$ bond that interchanges the two NH$_2$ groups. The DHFR–folate–NADP$^+$ complex at pH 5.3 showed a different set of H$^\eta$ signals for Arg 57 (see Table 1): these could be assigned to a third conformation (Form I) of the complex, which is
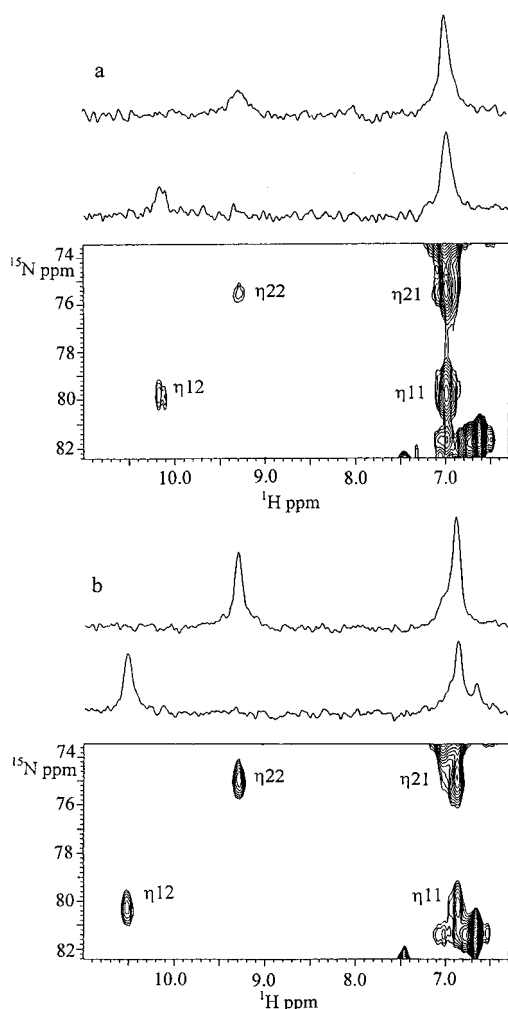
FIGURE 4: Part of the $^1H/^{15}N$ HSQC spectrum and the rows corresponding to the Arg 57 $^{15}N^\eta$ signals for complexes of *L. casei* DHFR with (a) *p*-aminobenzoyl-L-glutamate (PABG) and (b) PABG plus 2,4-diaminopyrimidine (DAP). Complexes were formed in the presence of excess PABG and DAP (1.0 mM DHFR, 4.4 mM PABG, and 1.1 mM DAP), and the 500-MHz spectra were recorded at 1 °C.

dominant at lower pH. At this temperature, there was no evidence of exchange between the three forms in zz-HSQC spectra recorded at pH values where all three forms coexist (rates of <6 s^{-1} would be difficult to detect in this experiment). Although the Arg 57 H$^\eta$ signals have different chemical shifts in the three forms, the chemical shift differences between the different forms are fairly small, and the chemical shifts are quite similar to those measured for the DHFR−methotrexate complex (see Table 1). For the binary complex of DHFR−folate at pH 7.3, the Arg 57 H$^\eta$ signals are also detected as two sets of resolved resonances with similar chemical shifts to those of the DHFR−methotrexate complex (see Table 1).

Complexes of DHFR with PABG and DAP. The $^1H/^{15}N$ HSQC spectra for the binary complex DHFR−PABG and the ternary complex DHFR−PABG−DAP are shown in Figure 4, panels a and b, respectively. These complexes were formed by titrating the DHFR sample with concentrated solutions of the ligands (see Materials and Methods). In the titration with PABG, all four H$^\eta$ signals were clearly visible in the spectra recorded at 2.4 to 7.9 equiv of PABG where they appeared with constant chemical shifts (as reported in

Table 1). The low field H$^\eta$ signals increase in intensity as the PABG concentration is increased (up to 7.8 equiv of PABG) and show essentially no change in the ^1H or ^{15}N chemical shifts. This clearly demonstrates that these Arg 57 H$^\eta$ signals are in slow exchange on the chemical shift timescale in both dimensions. The low field signals sharpen in the ^1H dimension on lowering the temperature: this further confirms the slow exchange between bound and free species. The high field signals were detected earlier in the titration than the low field signals (at 0.46 equiv of PABG), which suggests that the high field ^1H signals result from a fast exchange between bound and free protein. The high field signals sharpen in the ^1H dimension as the temperature is increased as expected for fast exchange. However, because the chemical shifts do not change during the titration, the ^1H chemical shifts differences between bound and free must be very small for the high field NH$^\eta$ signals. All four H$^\eta$ signals detected for Arg 57 for the DHFR−PABG complex have very similar $^1H/^{15}N$ chemical shifts to the corresponding signals in the DHFR−folate complexes (see Table 1).

In the presence of DAP, PABG binds 50 times more tightly to DHFR (*14, 15*). At 1 °C and 4.4 equiv of PABG and an excess of DAP, the DHFR is almost completely covered by both ligands. The $^1H/^{15}N$ HSQC spectrum shows four sharp H$^\eta$ signals of equal intensity for Arg 57, and these also have very similar chemical shifts to the corresponding signals in the DHFR−folate complexes (see Table 1).

Rates of N$^\epsilon$−C$^\zeta$ and C$^\zeta$−N$^\eta$ Bond Rotations. The N$^\epsilon$−C$^\zeta$ bond rotation rates were all obtained from zz-HSQC measurements and gave values that are fairly similar for all the complexes (12−31 s^{-1} at 1 °C, see Table 2).

For the DHFR−PABG complex, where a large population of free protein is present, a line shape analysis of the H$^\eta$ signals based on a three-site exchange model involving protons in an NH$_2$ group in their free and bound state was carried out (*23, 24*). From this analysis, both the dissociation rate and the C$^\zeta$−N$^\eta$ bond rotation rate were estimated to be <200 s^{-1} at 1 °C. For the other complexes, line shape analyses of the H$^\eta$ proton signals based on a two-site exchange between the NH$_2$ protons (H$^{\eta 11}$ and H$^{\eta 12}$) were carried out to provide upper limits for the C$^\zeta$−N$^\eta$ bond rotation rates (ranging from 50 to 90 s^{-1} at 1 °C). Because rotation about this bond is very fast in free arginine (see Table 2), the measured value in each complex will reflect the upper limit of the microscopic dissociation rate for the interaction between the arginine guanidino NH$_2$ group and the ligand α-glutamate carboxylate group.

DISCUSSION

Protein Environment of the Side Chain of Arg 57. In separate structural studies on complexes of DHFR with methotrexate, trimethoprim, trimetrexate (*27−30*), and NADPH (Polshakov, V. I., Birdsall, B., and Feeney, J., unpublished results), it was found that the side chain of Arg 57 is in the same position in all the structures with the arginine H$^\epsilon$ forming hydrogen bonds with the carbonyl oxygen of Pro 55 (distance about 2.0 Å) and probably also with the carbonyl oxygen of Leu 54 (distance around 2.4 Å) regardless of whether a ligand carboxylate group is interacting with the guanidino group. Further evidence for the hydrogen bonding to H$^\epsilon$ comes from its atypical chemical shifts and from the

observation of very slow H to D exchange rates for Arg 57 H^ϵ in all the complexes and also in apo DHFR. For apo DHFR, the Arg 57 H^ϵ chemical shift has the atypical value of 6.05 ppm and has very similar values in the spectra of the DHFR complexes with trimethoprim, trimetrexate, and NADPH (5.95, 6.02, and 6.02 ppm), where H^ϵ is known to have the hydrogen bonding interactions to Leu 54 and Pro 55. For complexes where a carboxylate group also interacts with Arg 57 (such as in DHFR−MTX), there is only a small shift for the H^ϵ (to 5.65 ppm) indicating that the H^ϵ proton is not greatly influenced by the H^η interactions with the carboxylate group. Thus in complexes such as DHFR−NADPH (and probably for apo DHFR) where the folate binding site is unoccupied, the presence of the H^ϵ hydrogen bonding ensures that the side chain of Arg 57 is already oriented in a way such that it can make good interactions with the ligand glutamate α-carboxylate group without requiring significant displacement of the side chain.

The Folate Glutamate Moiety Binds to Arg 57 in DHFR with a Symmetrical End-On Interaction and Binds in the Same Way in the Different Forms of the Folate and Folate−NADP$^+$ Complexes. The similar chemical shifts seen for the Arg 57 H^η signals observed for the methotrexate and folate complexes indicate that the α-carboxylate group of the ligand glutamate moiety interacts with the Arg 57 guanidino group in a similar way in the different complexes. In earlier work (*5*), it was shown that the only way in which a carboxylate group can interact with the H^η protons of Arg 57 to produce the large deshielding of the two centrally situated $H^{\eta 12}$ and $H^{\eta 22}$ protons is for the carboxylate oxygen atoms to form hydrogen bonds with these hydrogens in a symmetrical end-on manner described as a type 1 interaction by Lancelot and coworkers (*31*) and shown in Figure 2. In an analysis of arginine−aspartate interactions found in X-ray structures of proteins by Mitchell and coworkers (*32*), such an symmetrical end-on structure was found to be one of the most favored orientations for intermolecular interactions between arginine guanidino NH_2 and carboxylate groups. This model is fully consistent with the large downfield shifts seen for the Arg 57 $H^{\eta 12}$ and $H^{\eta 22}$ signals seen for the complexes of DHFR containing methotrexate or folate (see Figure 1, panels a and b and Table 1).

Furthermore, the similar chemical shifts observed for the Arg 57 N^η and H^η nuclei in the different conformations of the folate complexes (Forms I, IIa, and IIb) indicate that the glutamic acid moiety of folate is binding in a similar fashion in the different conformations (see Table 2 and Figure 1b). This agrees with earlier studies in which it was noted that His 28 of DHFR changes its pK by equal amounts in the different folate conformations: an increase in pK of His 28 by ∼1 unit results from the γ-carboxylate group of the glutamate moiety binding to His 28 (*33*, *34*). The major differences between the three forms of the folate complexes result from differences in the orientation of the pterin ring (∼180° different between Form IIb and Forms I and IIa) and in the charge/tautomeric states of the pterin ring (*25*, *26*). Despite these major differences in the pterin-binding site, it is clear that the glutamate interactions with His 28 and Arg 57 are the same in the different forms.

The Glutamate Moiety of the PABG Fragment Binds to Arg 57 of DHFR with an Almost Identical Symmetrical End-On Interaction to that Found in the DHFR−Folate and DHFR−Folate−NADP$^+$ Complexes. Arginine H^η chemical shifts are expected to be very sensitive to the lengths of the hydrogen bonds formed by the H^η protons with the oxygen of a ligand carboxylate group (*6*, *35*). Thus, the very similar Arg 57 H^η chemical shifts observed for DHFR complexes with PABG and those with the substrate folate indicate that the α-carboxylate group of the glutamate moiety is binding in an essentially identical manner to Arg 57 in the different complexes and with very similar hydrogen bond lengths and energies for the interactions. Earlier studies (*36*) had shown that the γ-carboxylate group of glutamate in PABG and folate also bind in a similar manner (in this case both increasing the pK value of His 28 by ∼1 pK unit). Thus the PABG glutamate moiety binds to DHFR in almost exactly the same way as does the folate glutamate with the α-carboxylate group binding to Arg 57 and the γ-carboxylate group binding to His 28.

Use of Arg 57 NH Signals for Monitoring Protein−Ligand Interactions with New Antifolates. The measured ^{1}H and ^{15}N chemical shifts of the Arg 57 guanidino NH signals for DHFR complexes with the substrate folate can be considered as characteristic values expected on formation of "optimized" interactions with a ligand carboxylate group. This pattern of shifts provides a target for use in monitoring the presence and quality of these interactions in complexes with new antifolate analogues containing carboxylate groups. In earlier NMR studies of DHFR complexes formed with brodimoprim analogues having carboxylate containing side chains (*6*), the changes in the Arg 57 H^η signals accompanying ligand binding indicated that one of the ligand carboxylate groups binds to Arg 57. However, the observed downfield shifts for $H^{\eta 12}$ and $H^{\eta 22}$ were much smaller than those seen in the DHFR−folate complexes (see Table 1), indicating that the interactions could probably be optimized by further modifications of the side chains.

Hindered Rotation in the Arg 57 Guanidino Group and Correlated Motion with the Ligand. At 1 °C, all the complexes examined showed four resolved Arg 57 H^η signals in their ^{1}H/^{15}N HSQC spectra indicating hindered rotation about the N^ϵ−C^ζ and C^ζ−N^η bonds. Thus, even for the most weakly binding ligand, PABG, [K_a 8.1×10^2 M^{-1} (*15*)] the interactions of the glutamate α-carboxylate with the Arg 57 guanidino group are sufficiently strong to induce hindered rotation. Interestingly, the rate of rotation about the N^ϵ−C^ζ bond in the complexes with the PABG binding fragment [for example, in the DHFR−PABG−DAP complex (13 ± 2 s^{-1}; K_a PABG 6.0×10^4 M^{-1} (*14, 15*)] is almost identical to those measured in the complex with the much more tightly binding methotrexate [14 ± 2 s^{-1}; K_a 2×10^9 M^{-1} (*14, 37*)] and fairly similar to those measured in the DHFR−MTX−NADPH complex [17 ± 4 s^{-1}; K_a MTX 1.2×10^{12} M^{-1} (*38*)] and in folate-containing complexes [12 to 31 s^{-1}; K_a 1 $\times$ 10^5 to 2×10^6 M^{-1} (*37, 38*)]. Previous studies on methotrexate complexes had indicated that this rotation does not require breakage of bonds between the ligand carboxylate group and the arginine guanidino H^η protons but rather depends on correlated rotations about the N^ϵ−C^ζ bond of Arg 57 and the C'−C^α bond of the glutamate α-carboxylate group of the ligand. The presence of correlated motions in PABG-containing complexes cannot be demonstrated directly (for the MTX complex, the necessary experiment to see the reversal of the rates of N^ϵ−C^ζ and C^ζ−N^η bond rotation

required a temperature of 40 °C, and such experiments are not possible for the PABG-containing complexes because of sample instability). However, it seems likely that these correlated motions will be present in all these complexes because the $N^\epsilon - C^\zeta$ bond rotation rates are remarkably similar in the PABG-containing and methotrexate complexes. This would mean that the α-carboxylate group in a fragment (such as PABG) is binding to the enzyme in a similar way to the carboxylate groups in parent molecules such as folate and methotrexate, thus leading to the correlated rotations being essentially the same in the different complexes.

From line shape analyses, the $C^\zeta - N^\eta$ bond rotation rates were estimated to be <200 s^{-1} in all the complexes examined. These bond rotations will depend on the rates of breaking of the hydrogen bonds. Our results can be considered in the context of our previously discussed model of dynamic processes within a protein ligand complex where we found that separate parts of a bound ligand can make and break its interactions with the protein many times within the lifetime of the complex (*39*). Thus, for example, the glutamate α- and γ-carboxylate groups would be expected to break their interactions with Arg 57 and His 28 several times (and not necessarily simultaneously) during the lifetime of the DHFR complex whether it be with PABG, folate, or methotrexate. At 1 °C, the microscopic rates of dissociation for the glutamate α-carboxylate group interaction with H$^\eta$ of Arg 57 are <200 s^{-1} for all the complexes studied regardless of their binding constants. However, a more detailed comparison of the complexes would require determination of the actual rates of rotation for the $C^\zeta - N^\eta$ bonds rather than upper limits.

It is clear that results from detailed NMR studies of specific protein−ligand interactions of the type discussed here can complement conventional structural information and thus provide a more complete understanding of the interactions and dynamics in protein−ligand complexes.

ACKNOWLEDGMENT

REFERENCES

1. Glushka, J., Barany, F., and Cowburn, D. (1989) *Biochem. Biophys. Res. Commun. 164*, 88−93.
2. Passcal, S. M., Yamazaki, T., Singer, A. U., Kay, L. E., and Forman-Kay, J. D. (1995) *Biochemistry 34*, 11353−11362.
3. Yamazaki, T., Pascal, S. M., Singer, A. U., Forman-Kay, J. D., and Kay, L. E. (1995) *J. Am. Chem. Soc. 117*, 3556−3564.
4. Feng, M.-H., Philippopoulos, M., MacKerell, A. D., Jr., and Lim, C. (1996) *J. Am. Chem. Soc. 118*, 11265−11277.
5. Gargaro, A. R., Frenkiel, T. A., Nieto, P. M., Birdsall, B., Polshakov, V. I., Morgan, W. D., and Feeney, J. (1996) *Eur. J. Biochem. 238*, 435−439.
6. Morgan, W. D., Birdsall, B., Nieto, P. M., Gargaro, A. R., and Feeney, J. (1999) *Biochemistry 38*, 2127−2134.
7. Nieto, P. M., Birdsall, B., Morgan, W. D., Frenkiel, T. A., Gargaro, A. R., and Feeney, J. (1997) *FEBS Lett. 405*, 16−20.
8. Bolin, J. T., Filman, D. J., Matthews, D. A., Hamlin, R. C., and Kraut, J. (1982) *J. Biol. Chem. 257*, 13650−13662.
9. Smith, R. J., Williams, D. H., and James, K. (1989) *J. Chem. Soc. Chem. Commun.* 682−683.
10. Henry, G. D., and Sykes, B. D. (1995) *J. Biomol. NMR 5*, 59−66.
11. Andrews, J., Clore, G. M., Davies, R. W., Gronenborn, A. M., Gronenborn, B., Kalderon, D., Papadopoulos, P. C., Schafer, S., Sims, P. F. G., and Stancombe, R. (1985) *Gene 35*, 217−222.
12. Dann, J. G., Ostler, G., Bjur, R. A., King, R. W., Scudder, P., Turner, P. C., Roberts, G. C. K., Burgen, A. S. V., and Harding, N. G. L. (1976) *Biochem. J. 157*, 559−571.
13. Roberts, G. C. K., Feeney, J., Burgen, A. S. V., Yuferov, V., Dann, J. G., and Bjur, R. (1974) *Biochemistry 13*, 5351−5357.
14. Birdsall, B., Burgen, A. S. V., Rodrigues de Miranda, J., and Roberts, G. C. K. (1978) *Biochemistry 17*, 2102−2110.
15. Birdsall, B., Burgen, A. S. V., and Roberts, G. C. K. (1980) *Biochemistry 19*, 3732−3737.
16. Sklenar, V., Piotto, M., Leppik, R., and Sauder, V. (1993) *J. Magn. Reson., Ser. A 102*, 241−245.
17. Shaka, A. J., Barker, P. B., and Freeman, R. (1985) *J. Magn. Reson. 64*, 547−552.
18. States, D. J., Haberkorn, R. A., Ruben, D. J. (1982) *J. Magn. Reson. 48*, 286−292.
19. Mori, S., Abeygunawardana, O'Neil Johnson, M., and Van Zijl, P. C. M. (1995) *J. Magn. Reson., Ser. B 108*, 94−98.
20. Wagner, G., Bodenhausen, G., Muller, N., Rance, M., Sorensen, O. W., Ernst, R. R., and Wuthrich, K. (1985) *J. Am. Chem. Soc. 107*, 6440−6446.
21. Wider, G., Neri, D., and Wuthrich, K. (1991) *J. Biomol. NMR 1*, 93−98.
22. Yamazaki, T., Pascal, S. M., Singer, A. U., Forman-Kay, J. D., and Kay, L. E. (1995) *J. Am. Chem. Soc. 117*, 3556−3564.
23. Sandström, J. (1982) *Dynamic NMR Spectroscopy*, Academic Press, London.
24. Polshakov, V. I., Birdsall, B., and Feeney, J. (1999) *Biochemistry 38*, 15962−15969.
25. Birdsall, B., Feeney, J., Tendler, S. J. B., Hammond, S. J., and Roberts, G. C. K. (1989) *Biochemistry 28*, 2297−2305.
26. Cheung, H. T. A., Birdsall, B., Frenkiel, T. A., Chau, D. D., and Feeney, J. (1993) *Biochemistry 32*, 6846−6854.
27. Martorell, G., Gradwell, M. J., Birdsall, B., Bauer, C. J., Frenkiel, T. A., Cheung, H. T. A., Polshakov, V. I., Kuyper, L., and Feeney, J. (1994) *Biochemistry 33*, 12416−12426.
28. Morgan, W. D., Birdsall, B., Polshakov, V. I., Sali, D., Kompis, I., and Feeney, J. (1995) *Biochemistry 34*, 11690−11702.
29. Gargaro, A. R., Soteriou, A., Frenkiel, T. A., Bauer, C. J., Birdsall, B., Polshakov, V. I., Barsukov, I. L., Roberts, G. C. K., and Feeney, J. (1998) *J. Mol. Biol. 277*, 119−134.
30. Polshakov, V. I., Birdsall, B., Frenkiel, T. A., Gargaro, A. R., and Feeney, J. (1999) *Protein Sci. 8*, 1−15.
31. Lancelot, G., Mayer, R., and Helene, C. (1979) *J. Am. Chem. Soc. 101*, 1569−1576.
32. Mitchell, J. B. O., Thornton, J. M., Singh, J., and Price, S. L. (1992) *J. Mol. Biol. 226*, 251−262.
33. Antonjuk, D. J., Birdsall, B., Burgen, A. S. V., Cheung, H. T. A., Clore, G. M., Feeney, J., Gronenborn, A., Roberts, G. C. K., and Tran, W. (1984) *Br. J. Pharmacol. 81*, 309−315.
34. Birdsall, B., Feeney, J., Pascual, C., Roberts, G. C. K., Kompis, I., Then, R. L., Muller, K., and Kroehn, A. (1984) *J. Med. Chem. 23*, 1672−1676.
35. Sternberg, U., and Brunner, E. (1994) *J. Magn. Reson. A 108*, 142−150.
36. Birdsall, B., Griffiths, D. V., Roberts, G. C. K., Feeney, J., and Burgen, A. S. V. (1977) *Proc. R. Soc. London B. 196*, 251−265.
37. Hood, K., and Roberts, G. C. K. (1978) *Biochem. J. 171*, 357−366.
38. Birdsall, B., Burgen, A. S. V., and Roberts, G. C. K. (1980) *Biochemistry 19*, 3723−3731.
39. Searle, M. S., Forster, M. J., Birdsall, B., Roberts, G. C. K., Feeney, J. Cheung, H. T. A., Kompis, I., and Geddes, A. J. (1988) *Proc. Nat. Acad. Sci. U.S.A. 85*, 3787−3791.